

Design of CLT Beams with Rectangular Holes or Notches

M. Flaig

Holzbau und Baukonstruktionen

Karlsruhe Institute of Technology, Germany

Keywords: cross laminated timber, beams, holes, notches, shear design, stress concentrations

1 Objectives and Scope

Beams with holes or notches are commonly used in modern timber structures. The areas around corners of holes and notches are subject to high shear stresses and tensile stresses perpendicular to the grain which severely decrease the load carrying capacity. In glulam beams the areas near holes and notches therefore usually need to be strengthened by means of screws or wood based panels. CLT beams with holes and notches, in contrast, do not need extra reinforcements since tensile forces perpendicular to the beam axis can be transferred by transversal layers that are included in the material. The work presented in this paper is intended to develop design rules for CLT members with holes and notches which at present do not exist in standards and approvals.

In CLT beams loaded in plane direction the crossing areas between longitudinal and transversal layers are subjected to torsional shear stresses and to shear stresses in direction of the beam axis which both result from transverse forces within the beam. In crossing areas near holes and notches both stress components are increased and tensile forces perpendicular to the beam axis cause additional shear stresses in transversal direction.

The design of CLT beams with holes and notches therefore requires *i)* suitable methods to determine the shear stress components in the crossing areas near the corners of holes and notches and *ii)* a failure criterion that takes into account the interaction of simultaneously occurring shear stress components.

In the first part of the presented work shear stresses in a large variety of CLT beams with holes and notches were determined by means of FE-calculations and the calculated values were used to derive stress concentration factors for a simplified design. The second part part of the work comprises tests with single crossing areas and bending tests with CLT beams with holes and notches. The test series with single crossing areas were designed to verify the failure criterions given in Eq. 1 that were derived from bending tests with prismatic CLT beams by Flaig and Blaß (2013) and take into account the linear interaction of parallel shear stress components at the edges of a crossing area.

$$\frac{\tau_{\text{tor}}}{f_{\text{v,tor}}} + \frac{\tau_{\text{yx}}}{f_{\text{R}}} \leq 1 \quad \text{and} \quad \frac{\tau_{\text{tor}}}{f_{\text{v,tor}}} + \frac{\tau_{\text{yz}}}{f_{\text{R}}} \leq 1 \quad \text{Eq. 1}$$

The main objectives of the bending tests were to determine the load carrying capacity of CLT beams with holes and notches and to investigate the structural behaviour and the failure modes. But the tests were also designed to check the approaches used for the calculation of internal stresses, especially the stress concentration factors obtained from FE calculations.

2 Calculation of stresses in CLT beams with holes and notches

2.1 Finite Element Model

In the FE-model used in this work longitudinal and transversal lamellae of CLT beams are represented by Timoshenko beam elements that are connected to each other via spring elements. The bending and the shear stiffness of the lamellae are represented by the beam elements while the stiffness of the glued connections between crosswise oriented lamellae is assigned to the spring elements. The modulus of elasticity and the shear modulus were assumed with 11,000 N/mm² and 690 N/mm², respectively, and the spring constants were calculated from the expressions given in Eq. 2 with a slip modulus $K = 7.5 \text{ N/mm}^3$ that was derived from the tests described in section 3.1.

$$K_x = K_y = K \cdot A_{CA} \quad \text{and} \quad K_\phi = K \cdot I_{p,CA} \quad \text{Eq. 2}$$

In contrast to the actual situation in CLT where longitudinal and transversal lamellae are continuously connected to each other the beam elements in the FE-model only have punctiform connections. The resulting free length between the nodes allows for additional bending and shear deformation in the beam elements which does not exist in reality. Consequently, some stiffness properties of transversal beam elements had to be modified to be more consistent with the real conditions:

- i.) a very high bending stiffness was assigned to beam elements representing transversal lamellae
- ii.) beam elements representing longitudinal and transversal lamellae were assigned the shear stiffness that was calculated with the gross thickness of the simulated CLT beams

Figure 1 shows the basic structure of the model and examples of the two beam types.

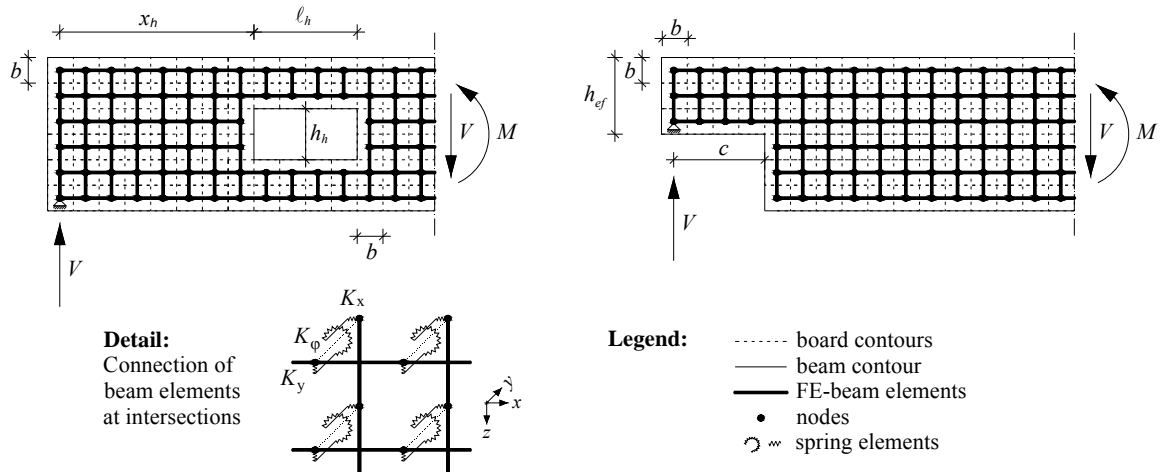


Figure 1: FE-model for the calculation of stresses in CLT beams with holes and notches

2.2 Stress Concentration Factors for CLT Beams with Holes

To determine stress concentration factors for CLT beams with holes the shear stresses in the crossing areas in the hole corners were calculated for beams and holes with various dimensions by means of the FE-model described in the previous section. In all simulated CLT beams the width of longitudinal and transversal lamellae was set to 150 mm and ratios of $t_{\text{net,cross}}/t_{\text{gross}} = 0.20$ and $t_{\text{gross}}/n_{CA} = 50 \text{ mm}$ were consistently used. The height of the simulated beams varied between 600 and 1800 mm in steps of 150 mm corresponding to a number m of longitudinal lamellae in direction of the beam height between 4 and 12. Due to the discretisation in the model, the length and the width of the holes were also chosen as integer multiples of the board width b so that in all the simulated CLT beams the edges of holes coincided with the edges of lamellae (cf. Figure 1). The dimensions of the holes varied within

the ranges of $b \leq \ell_h \leq h$ (length of the hole), $b \leq h_h \leq 0.5 \cdot h$ (height of the hole) and $1 \leq \ell_h/h_h \leq 4$. For all simulated beams the ratios $k_{h,1}$ and $k_{h,2}$ between the maximum shear stress components at the hole and the shear stress components in an undisturbed beam of equal dimensions were calculated. To determine the functional relationship between the peak stresses and the beam geometry regression analyses were performed from which Eq. 3 and Eq. 4 were derived.

$$k_{h1} = \frac{\tau_{\text{tor},h}}{\tau_{\text{tor}}} = 1.81 \cdot \left(\frac{\ell_h}{h} \cdot \frac{h_h}{h - h_h} \right) + 1.14 \quad \text{Eq. 3}$$

$$k_{h2} = \frac{\tau_{\text{yx},h}}{\tau_{\text{yx}}} = 0.103 \cdot \left(\frac{h_h \cdot \ell_h}{h^2} \cdot m^2 \right) + 1.27 \quad \text{Eq. 4}$$

The regression equations describe the peak stresses with adequate precision as can be seen in the diagrams on the left side of Figure 2 where the stress concentration factors $k_{h,1}$ and $k_{h,2}$ obtained from FE calculations are plotted against the predicted values according Eq. 3 and Eq. 4. The diagrams on the right side show the stress concentrations factors calculated according the regression equations, Eq. 3 and Eq. 4, in dependence of the dimensions of the hole.

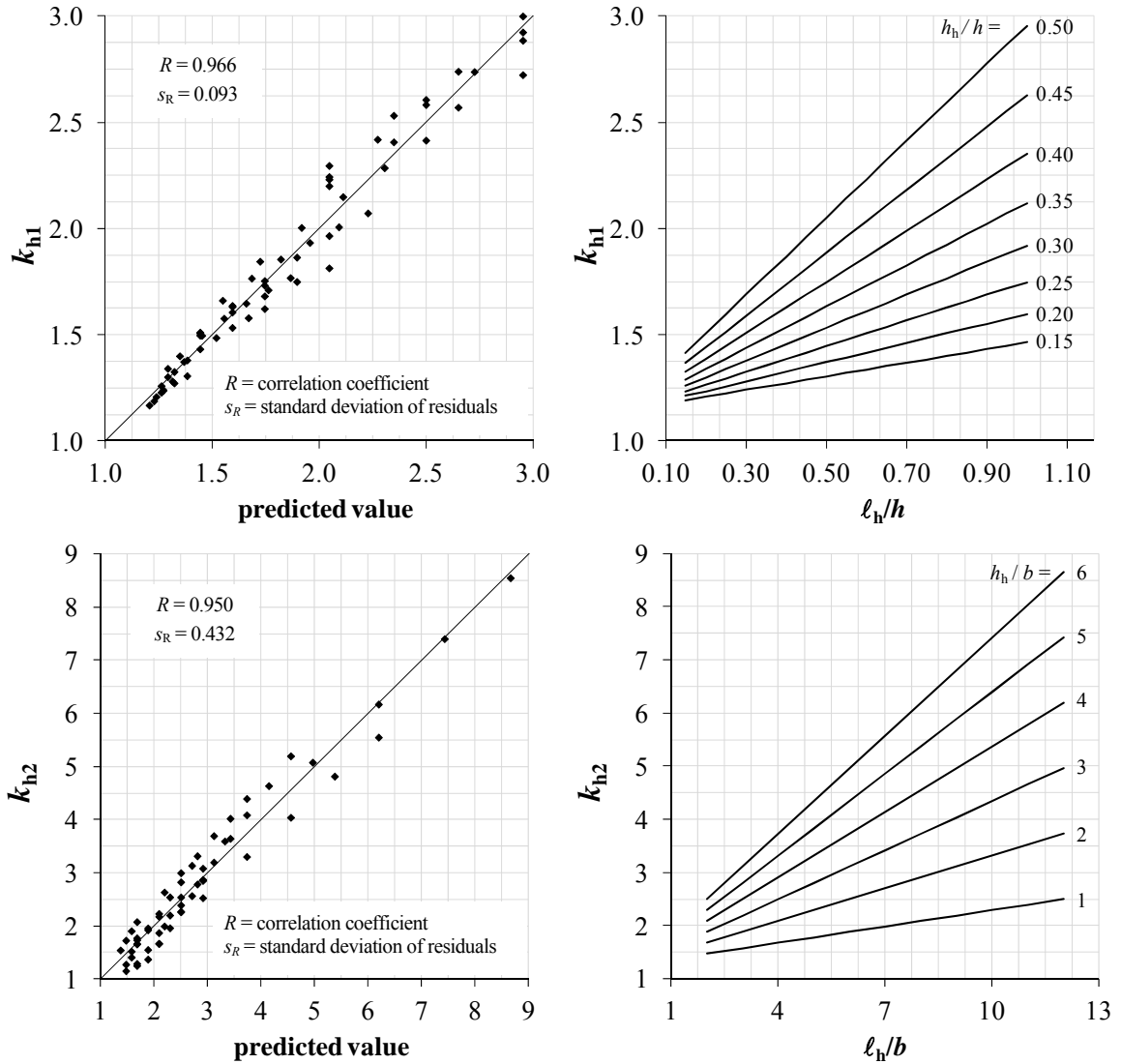


Figure 2: stress concentration factors for CLT beams with holes

The stress concentration factors depend on the ratio between the stiffness of the crossing areas and the stiffness of the lamellae which both are functions of different powers of the board width b . The above equations for the calculation of stress concentration factors are therefore

only valid for CLT beams consisting of lamellae with a width of 150 mm and should be adapted for board widths b differing from 150 mm. If the board width is within the range between 100 and 200 mm the multiplication with the factor k_b given in Eq. 5 provides good approximations for both factors k_{h1} and k_{h2} .

$$k_b = \left(\frac{b}{150} \right)^{1/3} \quad \text{Eq. 5}$$

2.3 Stress Concentration Factors for Notched CLT Beams

For notched CLT beams also stress concentration factors were determined by means of the FE-model described in section 2.1 using the same assumptions as for CLT beams with holes, i.e. the width of lamellae was set to 150 mm and ratios of $t_{\text{net,cross}}/t_{\text{gross}} = 0.20$ and $t_{\text{gross}}/n_{\text{CA}} = 50$ mm were used, consistently. The height of the simulated beams with notches was varied between 300 and 1200 mm. The height of the notch and the distance between the support and the corner of the notch varied between the width b of one lamella and half the beam height ($b \leq (h-h_{\text{ef}}) \leq 0.5 \cdot h$; $b \leq c \leq 0.5 \cdot h$). The ratio between the distance c and the reduced beam height h_{ef} was limited to values equal to or less than one ($c/h_{\text{ef}} \leq 1$). As for the holes the dimensions of the notches were chosen as integer multiples of the board width b so that the outlines of the notches coincided with the edges of lamellae (cf. Figure 1). In all simulated beams the shear stress component parallel to the beam axis in the crossing areas at the corner of the notch was smaller than the maximum shear stress component perpendicular to the beam axis. The determination of stress concentration factors for the shear stress component parallel to the beam axis was therefore omitted. To determine stress concentration factors k_n for the torsional shear stress component the ratio between the maximum stress in the corner of the notch and the corresponding value in a beam without notch was calculated for each simulated beam and a functional relationship between the peak stresses and the beam geometry was determined by means of a regression analysis.

$$k_n = 0.877 \cdot \left(\frac{h_{\text{ef}}}{h} \right)^{k_c} \quad \text{with } k_c = -1.81 \cdot \left(\frac{c}{h} \right)^{0.479} \quad \text{Eq. 6}$$

In Figure 3 on the left side the stress concentration factors k_n obtained from the FE calculations are plotted against the values predicted by the regression equation. In the diagram on the right side the values calculated according Eq. 6 are given in dependence of the dimensions of the notch.

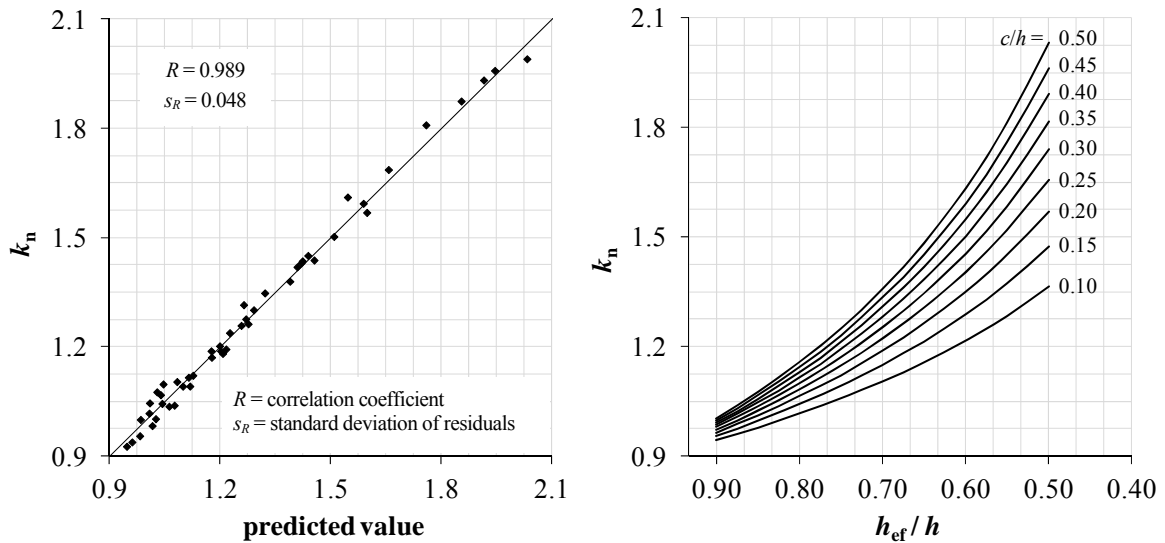


Figure 3: stress concentration factor for notched CLT beams

Due to the assumptions made in the FE model Eq. 6 for the calculation of the stress concentration factor k_n provides accurate results only for beams consisting of lamellae with a width of 150 mm. For beams with smaller or wider lamellae the factor k_n should be adjusted by multiplication with the factor k_b given in Eq. 5.

3 Experimental work

3.1 Single Crossing Areas under combined torsional and unidirectional shear stresses

3.1.1 Materials and Methods

Shear tests with single crossing areas were performed to verify the failure criterion given in Eq. 1. In four different test series the crossing areas of cross shaped specimens were subjected either to a shear force or to a torsional moment or to a combination of both loads. To make sure that the specimens of the different test series had equivalent material properties four sections were cut from one board at a time and then assembled in such a way that always four specimens, one for each series, consisted of sections of the same two boards. For testing, the specimens were fixed into a steel frame that consisted of two crosswise arranged bars as illustrated in Figure 4. The testing apparatus allowed applying arbitrary combinations of torsional and unidirectional shear stresses to the crossing areas by means of two independently controlled loads. Unidirectional rolling shear stresses were induced by a centrally applied vertical force F_v whereas torsional shear stresses were generated by an eccentric load F_{tor} acting at one end of the horizontal bar.

In the first test series (series V100) only a vertical shear force F_v was applied to determine the rolling shear strength of crossing areas as a reference value for the combined loading. In the second and the third series (series V50 and V35) load levels of about 50% and 35% of the mean value of the ultimate load determined in the first series were applied in combined loading. During the testing at first the shear force F_v was increased up to the defined level and kept constant. Only then the second load generating a torsional moment was applied and increased until failure. In the fourth series (series V0) the shear force F_v was set to zero and only a torsional moment was applied.

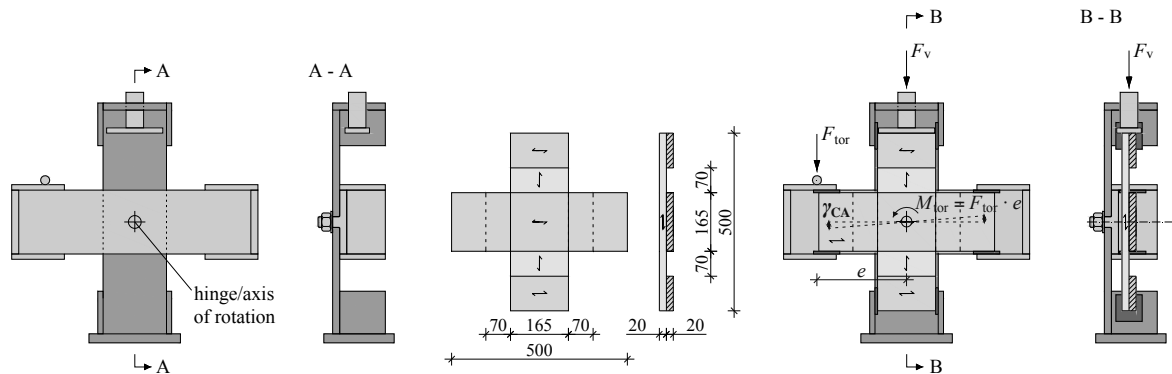


Figure 4: Testing apparatus, test specimens and test setup

3.1.2 Results

From the maximum values of the respective loads the rolling shear stresses and the torsional shear stresses were calculated. The mean values of shear stresses $\tau_{R,mean}$ and $\tau_{tor,mean}$, and the coefficients of variation are given in Table 1. In test series V100 and V0 where only one of the two loads, either shear force or torsional moment, had been applied, the evaluated stresses are the rolling shear strength or the torsional shear strength of the crossing areas, respectively. The mean values of the shear strength evaluated from these two test series were used to calculate the stress levels for all series. The calculated ratios between the actual shear stresses and the

mean values evaluated from Series V100 and V0 are plotted in the diagram shown in Figure 5. Due to the linear relationship which is clearly visible in the diagram the total utilisation rate η_{tot} for the test series V50 and V35 could be calculated as the sum of the two stress levels.

$$\eta_{\text{tot}} = \frac{\tau_{\text{tor}}}{f_{v,\text{tor,mean}}} + \frac{\tau_{\text{R}}}{f_{\text{R,mean}}} \quad \text{Eq. 7}$$

In Table 1 the shear strength properties of the two series with combined loading are given that were evaluated by multiplying the total utilisation rate with the mean values of shear strength obtained from series V100 and V0.

$$f_{\text{R},i} = \eta_{\text{tot}} \cdot f_{\text{R},\text{V100,mean}} \quad \text{and} \quad f_{v,\text{tor},i} = \eta_{\text{tot}} \cdot f_{v,\text{tor},\text{V0,mean}} \quad \text{Eq. 8}$$

Table 1: Mean values of shear stresses and shear strengths evaluated from tests with single crossing areas

Series		τ_{R}	f_{R}	τ_{tor}	$f_{v,\text{tor}}$
		in N/mm ²	in N/mm ²	in N/mm ²	in N/mm ²
V100	MEAN	1.26	-	-	-
	COV	0.158	-	-	-
V50	MEAN	0.66	1.29	1.51	3.07
	COV	0.013	0.17	0.34	0.17
V35	MEAN	0.46	1.28	1.94	3.03
	COV	0.002	0.14	0.22	0.14
V0	MEAN	-	-	2.97	-
	COV	-	-	0.09	-

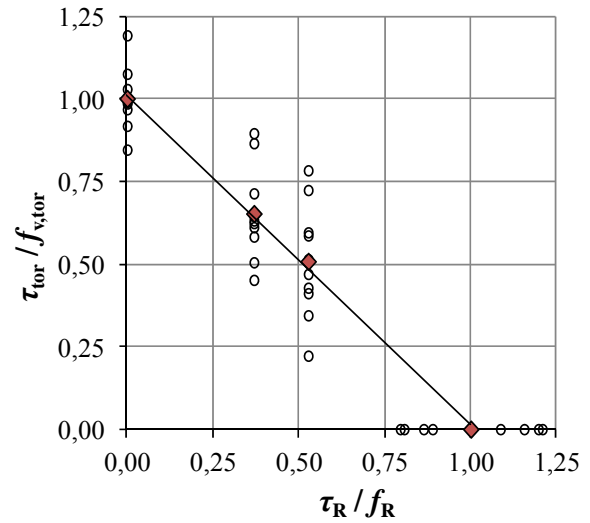


Figure 5: interaction of shear stresses in crossing areas

3.2 Beams with Holes

3.2.1 Materials and Methods

Ten CLT beams with holes were tested destructively to determine the load carrying capacity and to verify the stress concentration factors obtained from FE calculations. All specimens had the same outer dimensions and the same layout that consisted of four longitudinal and two transversal layers. The beams were divided in two series with holes of different height. The smaller holes had a height of 0.4 times the beam height which is the maximum allowable height of holes in glulam beams according to the German National Annex to EC5. The larger height was set to 0.5 times the beam height. In both series the length of the holes was equal to the beam height. In Table 2 the dimensions and the layout of the tested beams are quoted.

Table 2: Dimensions and layout of tested CLT beams with holes

Series	Number of specimens	dimensions in mm						layout
		h	t_{gross}	L	h_{h}	$h_{\text{ra/tb}}$	$t_{\text{long}} / t_{\text{cross}}$	
H40	5	600	150	6300	240	180	30/15	l-c-ll-c-l
H50	5	600	150	6300	300	150	30/15	l-c-ll-c-l

All specimens were produced from lamellae of strength class T14 according to EN 14080 with a width of 150 mm. The mean density was 459 kg/m³ in series H600-0.4 and 456 kg/m³ in series H600-0.5 at an average moisture content of 10.4% and 11.0%, respectively. The load carrying capacity of the beams was determined in four point bending tests with a span

of 10 times the beam height. The distance between the load application points was reduced to two times the beam height to avoid premature bending failure. The two holes were positioned in the middle between the loads and the supports and in the middle of the beam height. In Figure 6 the test setup and the beam geometry are illustrated.

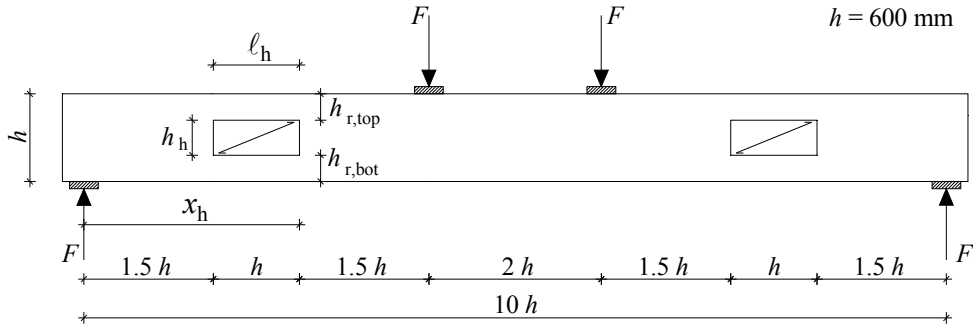


Figure 6: Test setup for beams with holes

3.2.2 Results

Two different types of failure were observed in both test series: Four of five specimens in each series failed due to shear stresses in the crossing areas near the corners of the holes. In the remaining two specimens failure was caused by bending stresses in the reduced cross section at the holes. In Figure 7 examples of the two observed types of failure are shown.



Figure 7: Shear failure in the crossing areas in specimen H50-4 (left), bending failure in the residual cross section below the hole in specimen H40-1 (right)

From the ultimate loads the bending stresses in longitudinal lamellae were evaluated in the middle of the span (Eq. 9) and at the edges of the holes farther from the supports (Eq. 10) where the additional bending moment resulting from the excentricity of shear forces was approximated as $M_V = V/2 \cdot \ell_h / 2$.

$$\sigma_{m,net} = \frac{24 \cdot F_{max}}{t_{net,long} \cdot h} \quad \text{Eq. 9}$$

$$\sigma_{m,net,h} = \frac{15 \cdot F_{max} \cdot h^2}{t_{net,long} \cdot (h^3 - h_h^3)} + \frac{3 \cdot F_{max} \cdot h}{2 \cdot t_{net,long} \cdot h_r^2} \quad \text{with } h_r = \min\{h_{r,top}, h_{r,bot}\} \quad \text{Eq. 10}$$

The tensile forces acting perpendicular to the beam axis at the vertical edges of the holes were calculated according Eq. 11 which is given in the German National Annex to EC5 for glulam beams with holes. A comparison with the results of FE calculations showed that Eq. 11 yields tensile forces that are slightly larger but still in good agreement with the values obtained from the FE model.

$$F_{t,90} = F_V + F_M = F_{max} \cdot \left[\left(\frac{3 \cdot h_h}{4 \cdot h} - \frac{h_h^3}{4 \cdot h^3} \right) + \left(\frac{0,008 \cdot x_h}{h_r} \right) \right]; \quad x_h \text{ cf. Figure 6} \quad \text{Eq. 11}$$

Tensile stresses in transversal lamellae at the edges of the holes were calculated using an effective width a_r which was assumed as the smaller value of the actual width of transversal lamellae and the maximum value given in the German National Annex to EC5 for reinforced holes in glulam beams with holes. The nonuniform distribution of tensile stresses within the effective width was taken into account by a factor $k_k = 2,0$ that was also adopted from the German National Annex to EC5.

$$\sigma_{t,0,cross} = k_k \cdot \frac{F_{t,90}}{a_r \cdot t_{net,cross}}; \text{ with } a_r = \min\{b_{cross}; 0.3 \cdot (h + h_h)\} \quad \text{Eq. 12}$$

In the evaluation of shear stresses three different failure modes were taken into account, i.e. shear stresses in the gross cross section (FM 1), shear stresses in the net cross section (FM 2) and shear stresses in the crossing areas (FM 3). A detailed description of the different failure modes and the calculation of shear stresses in prismatic CLT beams can be found in Flaig and Blaß (2013). In the tested CLT beams with holes the maximum values of shear stresses in the lamellae and in the crossing areas were calculated according to the equations given by Flaig and Blaß using either the residual cross section (FM 1) or the stress concentration factors k_{h1} and k_{h2} (FM 2 and FM 3) given in section 2.2. The shear stress component $\tau_{yz,h}$ perpendicular to the beam axis was calculated according Eq. 17 assuming a uniform distribution of shear stresses in the crossing areas within the effective length a_r (cf. Eq. 12) and the residual height h_r . In Table 3 the ultimate loads and the evaluated stresses are given.

$$\text{FM 1: } \tau_{xz,gross,h} = \frac{1.5 \cdot F_{max}}{(h - h_h) \cdot t_{gross}} \quad \text{Eq. 13}$$

$$\text{FM 2: } \tau_{xz,net,h} = k_{h2} \cdot \frac{1.5 \cdot F_{max}}{h \cdot t_{net}} \quad \text{Eq. 14}$$

$$\text{FM 3: } \tau_{tor,h} = k_{h1} \cdot \frac{3 \cdot F_{max}}{b^2 \cdot n_{CA}} \cdot \left(\frac{1}{m} - \frac{1}{m^3} \right) \text{ and} \quad \text{Eq. 15}$$

$$\tau_{yx,h} = k_{h2} \cdot \frac{6 \cdot F_{max}}{b^2 \cdot n_{CA}} \cdot \left(\frac{1}{m^2} - \frac{1}{m^3} \right) \text{ and} \quad \text{Eq. 16}$$

$$\tau_{yz,h} = \frac{F_{t,90}}{n_{CA} \cdot a_r \cdot h_r} \quad \text{where } h_r = \min \begin{cases} h_{r,top} \\ h_{r,bot} \end{cases} \quad \text{Eq. 17}$$

Table 3: Ultimate loads and evaluated stresses for tested CLT beams with holes (failure was caused by underlined stresses)

series	no.	F_{max} in kN	$\sigma_{m,net}$ in N/mm ²	$\sigma_{m,net,h}$ in N/mm ²	$\sigma_{t,0,cross}$ in N/mm ²	$\tau_{xz,gross,h}$ in N/mm ²	$\tau_{xz,net,h}$ in N/mm ²	$\tau_{tor,h}$ in N/mm ²	$\tau_{yx,h}$ in N/mm ²	$\tau_{yz,h}$ in N/mm ²
H40	1	93.8	31.3	<u>42.6</u>	14.6	2.61	15.9	1.52	0.76	0.30
	2	111	37.1	50.5	17.3	3.09	18.9	<u>1.81</u>	<u>0.91</u>	0.36
	3	112	37.3	50.8	17.4	3.11	19.0	<u>1.82</u>	<u>0.91</u>	0.36
	4	117	39.0	53.1	18.2	3.25	19.8	<u>1.90</u>	<u>0.95</u>	0.38
	5	115	38.4	52.4	18.0	3.20	19.5	<u>1.87</u>	<u>0.94</u>	0.37
H50	1	79.1	26.4	45.2	14.9	2.64	15.8	<u>1.58</u>	<u>0.75</u>	0.37
	2	93.4	31.1	53.4	17.6	3.11	18.6	<u>1.86</u>	<u>0.89</u>	0.44
	3	83.8	27.9	47.9	15.8	2.79	16.7	<u>1.67</u>	<u>0.80</u>	0.39
	4	95.0	31.7	54.3	17.9	3.17	18.9	<u>1.89</u>	<u>0.90</u>	0.45
	5	76.0	25.3	<u>43.4</u>	14.3	2.53	15.1	1.51	0.72	0.36

3.3 Notched CLT Beams

3.3.1 Materials and Methods

To determine the load carrying capacity of CLT beams with notches five specimens with equal were tested. The tested beams had a height of 600 mm and the layup consisted of four longitudinal and two transversal layers with a total thickness of 200 mm. The reduced height h_{ef} at the notched supports was half the beam height and the distance between the centre of the support and the corner of the notch was 300 mm. In Table 4 the dimensions and the layup of the tested beams are given in detail.

Table 4: Dimensions and layup of tested CLT beams with notches

No. of specimens	dimensions in mm						layup
	h	t_{gross}	L	h_{ef}	c	t_{long} / t_{cross}	
5	600	200	4800	300	300	40/20	l-c-ll-c-l

Like the tested beams with holes also the notched beams were produced from lamellae of strength class T14 with a width of 150 mm. In longitudinal lamellae the mean density was 425 kg/m^3 at an average moisture content of 12,0%. The beams had notched supports at both ends and were tested in four point bending tests with a span of 7.75 times the beam height. In Figure 8 the test setup used for the notched beams is illustrated.

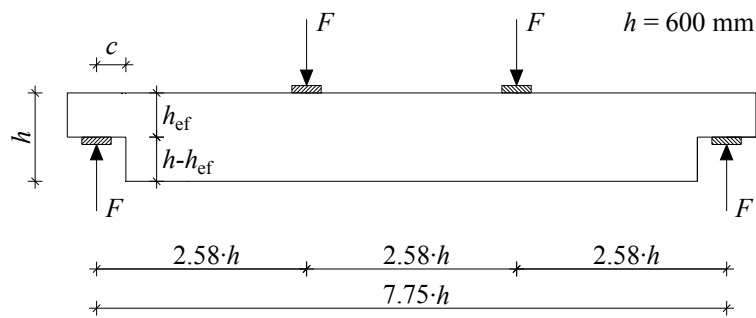


Figure 8: Test setup for notched beams

3.3.2 Results

In spite of the relatively low percentage of transversal layers of only 20% and the resulting high shear stresses in the net cross section of transversal layers (FM 2) failure was caused by shear stresses in the crossing areas in all specimens. Figure 9 shows an example of the failure mode observed.



Figure 9: Shear failure in the crossing areas next to the corner of the notch

From the ultimate loads the bending stresses in the middle of the span and in the reduced cross section at the notched support were calculated according Eq. 18 and Eq. 19. The tensile force perpendicular to the beam axis at the notch was calculated from Eq. 20 that is given in the

German National Annex to Eurocode 5 for notched glulam beams. Like the respective equation for beams with holes Eq. 20 yields tensile forces that are slightly larger than the values obtained from the FE calculations. The maximum tensile stresses in the transversal lamellae next to the notch were calculated according Eq. 21. The factor k_k in Eq. 21 takes into account the nonuniform stress distribution within the effective length ℓ_r . A value of $k_k = 2.0$ and the limitation of the effective length $\ell_r \geq 0.5 \cdot (h - h_{ef})$ were adopted from the design rules given in the German National Annex to Eurocode 5 for notched glulam beams. The results of FE calculations showed in addition that in CLT beams the complete tensile force $F_{t,90}$ acts in the transversal lamellae directly next to the notch so that in large CLT beams the effective length should be limited to the width of one transversal lamella.

$$\sigma_{m,net} = \frac{15 \cdot F_{max}}{t_{net,long} \cdot h} \quad \text{Eq. 18}$$

$$\sigma_{m,net,A} = \frac{6 \cdot c \cdot F_{max}}{t_{net,long} \cdot h_e^2} \quad \text{Eq. 19}$$

$$F_{t,90} = 1.3 \cdot F_{max} \cdot \left[3 \cdot \left(1 - \frac{h_{ef}}{h} \right)^2 - 2 \cdot \left(1 - \frac{h_{ef}}{h} \right)^3 \right] \quad \text{Eq. 20}$$

$$\sigma_{t,0,cross} = k_k \cdot \frac{F_{t,90}}{\ell_r \cdot t_{net,cross}}; \quad \text{with } \ell_r = \max \{ 0.5 \cdot (h - h_{ef}); b_{cross} \} \quad \text{Eq. 21}$$

As for beams with holes the shear stresses related to the three failure modes were evaluated from the maximum shear force F_{max} . In FM1, that takes into account shear stresses in the gross cross section (i.e. shear stresses act within the total thickness of a beam), the maximum shear stress occurs in the beam section with reduced height. The actual shear stress in the gross cross section of the test specimen was calculated according Eq. 22. In notched beams the maximum shear stresses in the net cross section (FM 2) arise in the corner of the notch. In the tested CLT beams the shear stresses in the net cross section of transversal layers were calculated from Eq. 23 with the full beam height h and a factor k_n according Eq. 6 taking into account stress concentrations in the corner of the notch. The maximum values of shear stresses in the crossing areas at the notched supports were calculated according Eq. 24 and Eq. 25. In Eq. 24 the increase of the torsional shear stress component in crossing areas next to the notch is again taken into account by the factor k_n according Eq. 6. The shear stress component perpendicular to the beam axis is calculated from the tensile force $F_{t,90}$ given in Eq. 20 assuming a uniform stress distribution within the effective length ℓ_r and the residual height h_n .

The evaluation of shear stresses in the crossing areas acting parallel to the beam axis was omitted since FE calculations and tests showed that this component is not decisive for the design. In Table 5 the ultimate loads reached in the tests and the evaluated bending and shear stresses are summarized.

$$\text{FM1: } \tau_{xz,gross,n} = \frac{1.5 \cdot F_{max}}{h_e \cdot t_{gross}} \quad \text{Eq. 22}$$

$$\text{FM2: } \tau_{xz,net,n} = k_n \cdot \frac{1.5 \cdot F_{max}}{h \cdot t_{net}} \quad \text{Eq. 23}$$

$$\text{FM3: } \tau_{tor,n} = k_n \cdot \frac{3 \cdot F_{max}}{b^2 \cdot n_{CA}} \cdot \left(\frac{1}{m} - \frac{1}{m^3} \right) \quad \text{Eq. 24}$$

$$\tau_{yz,n} = \frac{F_{t,90}}{n_{CA} \cdot \ell_r \cdot h_n}; \quad \text{where } h_n = \min \{ h_{ef}; h - h_{ef} \} \quad \text{Eq. 25}$$

Table 5: Ultimate loads and evaluated stresses for tested CLT beams with notches (failure was caused by underlined stresses)

series	no.	F_{\max} in kN	$\sigma_{m,net}$ in N/mm ²	$\sigma_{m,net,A}$ in N/mm ²	$\sigma_{t,0,cross}$ in N/mm ²	$\tau_{xz,gross,n}$ in N/mm ²	$\tau_{xz,net,n}$ in N/mm ²	$\tau_{tor,n}$ in N/mm ²	$\tau_{yz,n}$ in N/mm ²
N600	1	157	25.3	24.5	17.0	3.91	19.9	<u>2.48</u>	<u>0.57</u>
	2	162	26.2	25.4	17.6	4.06	20.6	<u>2.57</u>	<u>0.59</u>
	3	148	23.9	23.2	16.1	3.71	18.8	<u>2.35</u>	<u>0.54</u>
	4	148	23.9	23.2	16.1	3.71	18.8	<u>2.35</u>	<u>0.54</u>
	5	158	25.5	24.6	17.1	3.94	20.0	<u>2.50</u>	<u>0.57</u>

4 Summary and conclusions

In nearly all of the tested CLT beams with holes and notches failure was caused by shear stresses in the crossing areas which shows that an accurate calculation of these stresses as well as a basic understanding of the interaction of different stress components and the knowledge of strength properties of crossing areas are indispensable for a reliable and economic design.

The strength properties that were obtained from the described test series with single crossing areas are relatively low compared to the values determined in earlier studies but the ratio of the two shear strengths lies within the usual range of 2.25 to 2.5.

$$\frac{f_{v,tor,mean}}{f_{R,mean}} = \frac{2.97}{1.26} = 2.37 \quad \text{Eq. 26}$$

The torsional shear strength and the rolling shear strength that were evaluated for the test series with notched beams and beams with holes using the ratio given in Eq. 26 are somewhat larger than those determined for single crossing areas but agree very well with the strength properties of crossing areas found in earlier studies (cf. Table 6).

Together with the failure criterion that was derived from the tests with single crossing areas the equations and the stress concentration factors used for the calculation of shear stresses in the crossing areas of CLT beams with holes and notches provide an adequate design method for CLT beams with holes and notches.

Another finding of the performed test series with CLT beams is that the shear strength in sections through the unglued joints between the lamellae of one direction which is needed for the verification of shear stresses in the net cross section of CLT members is significantly larger than previously assumed.

Table 6: Shear strength properties of crossing areas

Test series	$f_{v,tor,mean}$ in N/mm ²	$f_{R,mean}$ in N/mm ²
This work	CLT Beams with Notches	3.78
	CLT Beams with Holes	3.54
	Single crossing areas	3.03
Earlier work	Blaß and Görlacher (2002)	3.59
	Jöbstl (2004)	3.46
	Wallner (2004)	-
	Blaß and Flaig (2013)	-

5 Symbols

A_{CA}	crossing area
b	width of lamellae
c	distance between the corner of a notch and the centre of the support
F_{max}	ultimate load
$F_{t,90}$	tensile force acting perpendicular to the beam axis
f_R	rolling shear strength
$f_{v,tor}$	torsional shear strength of crossing areas of orthogonally bonded lamellae
h	beam height
h_n	smaller height above or below the corner of a notch
$h_{r,top/bot}$	residual height above or below a hole
h_h	hole height
h_{ef}	reduced height at notched support
$I_{p,CA}$	polar moment of inertia of a single crossing area
K	slip modulus of crossing areas in N/mm per mm ²
k	factor
ℓ_h	length of hole
m	number of longitudinal lamellae within the beam height
n_{CA}	number of crossing areas within the beam thickness
t_{gross}	total thickness of a CLT beam
$t_{net,long}$	net thickness of longitudinal layers
t_{net}	smaller of the net thickness of longitudinal and the net thickness of transversal layers
η	stress level, utilisation rate
$\sigma_{t,0,cross}$	tensile stress in transversal layers
$\sigma_{m,net}$	bending stress in longitudinal layers
$\tau_{xz,gross}$	shear stress in the gross cross section
$\tau_{xz,net}$	shear stress in the net cross section
τ_{tor}	torsional shear stress in crossing areas
τ_{yx}	unidirectional shear stress acting parallel to the beam axis in crossing areas
τ_{yz}	unidirectional shear stress acting perpendicular to the beam axis in crossing areas

Indices

CA	crossing area
h	hole
n	notch
gross	related to the total thickness of a CLT beam
net	related to the net thickness; here: the sum of the thicknesses of transversal layers
long	related to longitudinal layers/lamellae
cross	related to transversal layers/lamellae

6 References

- Aicher, S. (2012): “Glulam beams with internally and externally reinforced holes – tests, detailing and design“ In: Proceedings. CIB-W18 Meeting 44, Alghero, Italy, 2011, Paper 44-12-4.
- Aicher, S.; Höfflin, L. (2010): “Glulam beams with holes reinforced by steel bars” In: Proceedings. CIB-W18 Meeting 42, Dübendorf, Switzerland, 2009, Paper 42-12-1.
- Bejtka, I.: “Cross (CLT) and diagonal (DLT) laminated timber as innovative material for beam elements”. Karlsruhe Berichte zum Ingenieurholzbau, Bd. 17, KIT Scientific Publishing, 2011
- Bogensperger, T.; Moosbrugger, T.; Silly, G.: “Verification of CLT-plates under loads in plane”. In: Proceedings. 11th World Conference on Timber Engineering, Riva del Garda, Italy, 2010
- Bogensperger, T.; Moosbrugger, T.; Schickhofer, G.: “New Test Configuration for CLT-Wall Elements under Shear Load”. In: Proceedings. CIB-W18 Meeting 40, Bled, Slovenia, 2007, Paper 40-12-3
- Bosl, R.: “Zum Nachweis des Trag- und Verformungsverhaltens von Wandscheiben aus Brettspertholz”. Dissertation, Universität der Bundeswehr, München, Germany, 2002
- Flaig, M.; Blaß, H.J.: “Shear Strength and Shear Stiffness of CLT beams Loaded in Plane” In: Proceedings. CIB-W18 Meeting 46, Vancouver, Canada, 2013, Paper 46-12-3
- Flaig, M.; Blaß, H.J.: “Bending Strength of Cross Laminated Timber Beams Loaded in Plane” In: Proceedings. World Conference on Timber Engineering (WCTE), Quebec, Canada, 2014
- Flaig, M.: „Biegeträger aus Brettspertholz bei Beanspruchung in Plattenebene“. Dissertation, Karlsruhe Berichte zum Ingenieurholzbau, Bd. 26, KIT Scientific Publishing, 2013
- Jockwer, R.: “Structural behaviour of glued laminated timber beams with unreinforced and reinforced notches” Dissertation, ETH Zurich, Switzerland, 2014
- Jöbstl, R.A.; Bogensperger, T.; Schickhofer, G.: “In-Plane Shear Strength of Cross Laminated Timber”. In: Proceedings. CIB-W18 Meeting 41, St. Andrews, Canada, 2008, Paper 41-12-3
- Jöbstl, R.A.; Bogensperger, T.; Schickhofer, G.: “Mechanical Behaviour of Two Orthogonally Glued Boards”. In: Proceedings. 8th World Conference on Timber Engineering, Lahti, Finland, 2004
- Moosbrugger, T.; Guggenberger, W.; Bogensperger, T.: “Cross Laminated Timber Wall Segments under homogeneous Shear — with and without Openings”. In: Proceedings. 9th World Conference on Timber Engineering, Portland, Oregon, USA, 2006
- Schickhofer et al.: “BSPhandbuch - Holz-Massivbauweise in Brettspertholz”. Technische Universität Graz, holz.bau forschungs gmbh, Karlsruher Institut für Technologie, Technische Universität München, Eidgenössische Technische Hochschule Zürich, 2009
- Traetta, G., Bogensperger, T., Schickhofer, G.: “Verformungsverhalten von Brettspertholzplatten unter Schubbeanspruchung in der Ebene”. In: 5. Grazer Holzbau-Fachtagung, September 2006